




REGULAR ARTICLE

Study of Optical Properties and Structural Features of Object using
the X-ray Phase Contrast Method

A.Yu. Ovcharenko* , O.A. Lebed

Institute of Applied Physics, National Academy of Sciences of Ukraine, 40007 Sumy, Ukraine

(Received 25 April 2024; revised manuscript received 20 June 2024; published online 28 June 2024)

Phase contrast is widely used in all fields for visualization of the internal structure of objects using X-ray radiation. The paper proposes a new approach to modeling a phase-contrast X-ray image by the method of free propagation using the Fresnel-Kirchhoff diffraction theory. A simple calculation model was developed, which makes it possible to determine the value of the change in the intensity of X-rays on three-dimensional models of objects of arbitrary shape with macroscopic dimensions. It also allows you to establish the conditions for observing a contrast image with known characteristics of the detector system and the intensity of the radiation source. The possibility of obtaining clear images of objects with small decrements of refraction of matter, determining their geometric dimensions and thickness was shown. A method of calculating the optical properties of metal alloys in the X-ray range has been developed. The approaches presented in the paper can be useful to developers of compact devices for detecting structural inhomogeneities inside the studied objects by a non-destructive method.

Keywords: X-ray phase contrast imaging, Radiation matter interaction, Non-destructive analysis, X-ray diffraction, Fresnel-Kirchhoff diffraction theory, Internal structure, Thermal expansion.

DOI: [10.21272/jnep.16\(3\).03028](https://doi.org/10.21272/jnep.16(3).03028)

PACS numbers: 42.25.Bs, 42.30.Va

1. INTRODUCTION

Controlling the quality and reliability of modern materials and products is a very urgent task in many branches of industry and scientific research. This is especially important in the transport, medical and energy sectors, where product failure can lead to man-made disasters and human casualties. Complex technical objects often have internal defects and structural inhomogeneities that cannot be detected by traditional control methods and significantly reduce the reliability and service life of structures.

Along with this, X-ray radiation is an important diagnostic tool in the field of biology and medicine. X-rays have a high penetrating ability for most materials and allow to study the internal structure of the object without destroying it. Most of the traditional methods of medical and industrial radiography, tomography, and microscopy are usually based on the change in the absorption coefficient of X-rays in different parts of the object due to changes in its density, composition, and thickness. This task is seriously complicated for the study of weakly absorbing objects (for example, soft biological tissues). Although X-rays penetrate deeply into such materials, the contrast of their images is weak due to the small value of the absorption coefficient. The use of hard X-ray radiation in tomography makes it possible to prevent its complete absorption and obtain information about the internal structure of larger objects in a non-destructive way. It follows that in order to reduce the radiation dose, it is necessary to develop methods based

on the refraction of X-rays. Therefore, the development of fundamentally new approaches to non-destructive testing is an important task of scientific and technical progress and the development of medicine.

One of the most promising methods in this field is phase X-ray tomography, which is based on the analysis of the spatial distribution of the phase of coherent radiation that passes through the object under study. Unlike conventional radiography, it provides a much higher sensitivity to internal inhomogeneities of the material at the micro- and submicron level, in particular, microcracks, pores, etc. Therefore, recently, phase X-ray tomography has been successfully used in the aerospace industry and mechanical engineering for express analysis of products and structures [1, 2]. It is also widely included in the arsenal of medical imaging tools due to the high contrast of soft tissues [3].

Research of relatively large biological objects by methods based on the phenomenon of absorption requires the use of hard radiation, the introduction of contrast agents and a larger dose of radiation. The X-ray phase contrast imaging (PCI) method allows one to visualize the internal structure of weakly absorbing objects with small substance density gradients with high spatial resolution. The basis of this method is the use of the phenomenon of refraction of X-rays in the object, which leads to a change in the phase front of the wave [3-10]. As a result of such a phase change, X-rays deviate from their primary direction by small angles, the value of which depends on the spatial distribution of the density of matter in the object. From the point of view of wave

* Correspondence e-mail: oartturr@gmail.com



optics, phase-contrast images are the result of the interference of the incident wave with the waves that have passed through the sample. The study of objects using methods based on the phenomenon of X-ray refraction is an urgent task for many areas of modern applied science and medicine.

Contrast images in X-ray radiation are considered promising technologies in medicine, which increases the contrast resolution of radiographic methods [3, 8]. This technology will improve the functioning of traditional X-ray computed tomography diagnostics and nuclear magnetic resonance scanning systems. PCI methods for applications in early diagnosis and medical imaging in the future will allow solving the main problems in this field: reducing the radiation dose, increasing the resolution and contrast for imaging soft tissues in the early stages of diseases.

In this paper, the propagation-based phase contrast method is considered as one of the most common methods of obtaining phase contrast images. For the first time, a similar scheme was used by Gabor in an electron microscope experiment [11] and was later developed as a phase contrast method in the X-ray range [5, 12-18]. An important advantage of this method is the simplicity of its experimental implementation, which does not require the use of complex X-ray optical elements.

However, the full and effective application of this method in practice requires significant improvements in both hardware and mathematical calculation models that describe the process of phase contrast formation. In particular, it is necessary to solve the issue of creating compact phase tomography devices by optimizing design parameters and operating modes based on simulation of physical processes. Currently, little attention is paid to this direction, so there are situational problems that need to be solved.

2. ANALYTICAL MODEL

The method of free propagation or in-line phase contrast is implemented in the field of Fresnel diffraction [3-6, 12, 18-22].

Internal variations in the thickness and index of refraction of X-ray rays of the investigated object lead to a change in the shape of the X-ray wavefront when passing through the object. When the detector is located directly behind the investigated object, we get a simple absorption X-ray image, and at significant distances from the object, a phase-contrast image in X-rays is formed. The optical properties of an object can be characterized by a complex index of refraction n :

$$n = 1 - \delta + i\beta, \quad (1)$$

where the value β is responsible for describing the absorption properties of the material under study (absorption index), and δ describes the phase shift of the wavefront caused by the passage of rays through the object.

The value of δ depends on the chemical composition, the electron density of the object's material, and the wavelength of the incident radiation. This parameter determines the phase shift and amplitude of the secondary waves scattered by the object, which significantly affects the diffraction pattern. Ignoring the decrement can lead to significant errors in calculations.

It is obvious that a change in the electron density will occur during mechanical deformation and this will lead to a change in the optical properties of the material under study. Let's get the ratio for the refraction decrement δ and the absorption coefficient β of the multicomponent alloy.

In the general case, the δ value can be calculated by the formula [23, 24]:

$$\delta = \frac{r_0 \lambda^2 n_e}{2\pi}, \quad (2)$$

where $r_0 = e^2/4\pi\epsilon_0 mc_0^2$ is the classical electron radius; n_e is electron density; e is electron charge; ϵ_0 is dielectric constant of vacuum; m is electron mass; c_0 is speed of light in a vacuum.

For crystalline samples in the formula (2), the electron density n_e is determined by the number of electrons z in one atom and the concentration of atoms n_a :

$$n_e = zn_a = z \frac{k_c}{V_c}, \quad (3)$$

where k_c , V_c is the number of atoms in one elementary cell and the volume of the elementary cell, respectively.

For a multicomponent alloy, where the concentration of components is equal to c_1, c_2, \dots, c_l , the formula (3) can be written:

$$n_e = \frac{k_c}{V_c} (z_1 c_1 + z_2 c_2 + \dots + z_l c_l), \quad (4)$$

where z_1, z_2, \dots, z_l are ordinal numbers of chemical elements that are components of the alloy, l is the number of elements in the alloy.

Substituting (4) into (2), we obtain an expression for the refractive index δ of an alloy with a uniform distribution of components over the crystal volume

$$\delta = \frac{e^2 \lambda^2 k_c}{8\pi^2 \epsilon_0 m c_0^2 V_c} (z_1 c_1 + z_2 c_2 + \dots + z_l c_l). \quad (5)$$

For a more accurate calculation of δ , the ordinal numbers z_1, z_2, \dots, z_l in the formula (5) should be replaced by the real part of the complex atomic form factor $f = z + f' + if''$ [24]:

$$\delta = \frac{e^2 \lambda^2 k_c}{8\pi^2 \epsilon_0 m c_0^2 V_c} \times [c_1(z_1 + f'_1) + c_2(z_2 + f'_2) + \dots + c_l(z_l + f'_l)]. \quad (6)$$

The absorption coefficient β is determined by the imaginary part f'' of the complex atomic form factor [24]:

$$\beta = \frac{e^2 \lambda^2 k_c}{8\pi^2 \epsilon_0 m c_0^2 V_c} f''. \quad (7)$$

The absorption coefficient of an alloy with a uniform distribution of components can be found as the sum of the absorption coefficients from each component:

$$\beta = \frac{e^2 \lambda^2 k_c}{8\pi^2 \epsilon_0 m c_0^2 V_c} [c_1 f''_1 + c_2 f''_2 + \dots + c_l f''_l]. \quad (8)$$

The phase shift of the X-ray wave that passed through the sample depends on the variations of the refraction decrement δ inside the sample and on its thickness. In the case of a monochromatic wave propagating along the z axis, the phase shift can be written in the following form [24]:

$$\varphi(x, y) = -\frac{2\pi}{\lambda} \int \delta(x, y, z) dz, \quad (9)$$

where the integral is calculated over the thickness of the object in the direction of propagation of the X-ray beam. Later, formula (9) will be used to calculate the phase shift during the passage of X-rays through the samples.

In this work, the Fresnel-Kirchhoff scalar diffraction theory is used as the basis of the calculation model for the calculation of phase-contrast images. This makes it possible to take into account the evolution of the wave front on the path "source – object" and "object – screen".

The Figure 1 schematically shows the path of rays from the X-ray source to the screen through the object under study. This approach is quite general and is suitable for calculating diffraction patterns both from point sources of radiation and for extended ones. In addition, it is possible to perform a numerical experiment for objects of any geometric shape from mesoscopic to macroscopic scales.

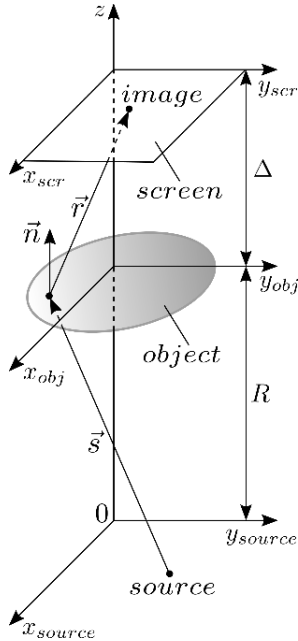


Fig. 1 – The scheme of calculating the phase contrast image in the Fresnel-Kirchhoff diffraction theory

For the case of an X-ray beam propagating from a point source, the expression for the intensity in the plane of the detector can be written in the form [18, 24]:

$$\psi(x_{scr}, y_{scr}) = \frac{1}{i\lambda} \iint_{-\infty}^{\infty} \frac{\exp(ik(r+s))}{2rs} \times$$

$$\times (\cos(\mathbf{n}, \mathbf{r}_i) + \cos(\mathbf{n}, \mathbf{s}_i)) \cdot \exp(i\varphi) \cdot dx_i dy_i, \quad (10)$$

$$s = \sqrt{(x_i - x_s)^2 + (y_i - y_s)^2 + R^2}, \quad (11)$$

$$r = \sqrt{(x_i - x_{scr})^2 + (y_i - y_{scr})^2 + \Delta^2}. \quad (12)$$

Here \vec{s} and \vec{r} are "source – object" and "object – screen" vectors, respectively; λ is wavelength of radiation; \vec{n} is normal to the plane of the object; φ is additional phase shift caused by the impact of the object on the incoming wavefront.

3. RESEARCH METHODOLOGY

Currently, there is a very small number of works on

computer modeling of X-ray diffraction on various objects, and this, in our opinion, is explained by several reasons. First, this kind of modeling requires the availability of sufficiently powerful computing resources, since the correct calculation of the integral according to the formula (10) can be carried out only by numerical methods when dividing the object plane and the screen plane into a very large number of points and with using double precision when calculating all values that are included in this formula. This, in turn, leads to problems of processing experimental data in real time. Secondly, although the above-mentioned model is quite universal and does not contain restrictions on the size and geometric shape of the studied objects, it is quite difficult to model volumetric objects of irregular geometric shape. In this regard, as a rule, modeling is carried out for very simple objects under the assumption that their dimensions are much smaller than the distance from the source to the object and have a certain symmetry. The thickness of the objects was simply set analytically, which is a significant limitation when conducting similar studies.

The application of the scalar theory of Fresnel-Kirchhoff diffraction allowed us to develop an approach for modeling X-ray diffraction from models of real three-dimensional objects of any geometric shape. Figure 2 shows the scheme for calculating the thicknesses of the investigated objects and phase shifts of X-ray waves, which was implemented in our work. For this, a three-dimensional object was defined as a geometric position of points that forms its surface. Further, the wave front, after passing through the test sample, was divided into a large number of points, and a straight line was drawn from the radiation source to each of these points. Using the equation of the straight line and coordinates of the points of the object, the intersection points (x_1, y_1, z_{min}) and (x_2, y_2, z_{max}) were determined and the thickness of the object was calculated $d_1 = \sqrt{(x_2 - x_1)^2 + (y_2 - y_1)^2 + (z_{max} - z_{min})^2}$ and phase shift $\varphi = k\delta d_1$, where δ is index of refraction.

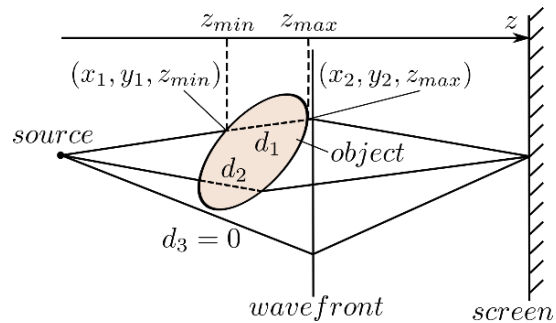


Fig. 2 – Scheme for calculating sample thicknesses and X-ray phase shifts

4. RESULTS AND DISCUSSION

The presented study is part of the work on X-ray phase contrast experiments within the framework of the Associated International Laboratory LIA/IRP IDEATE [25, 26]. A point source with a wavelength of $\lambda = 1.5 \cdot 10^{-4} \mu\text{m}$, which corresponds to the characteristic line of $\text{CuK}\alpha$, was accelerated. We chose the object

shown in the Figure 3 as the studied sample. Its maximum geometric dimensions along the x , y , and z axes were respectively equal to $100\ \mu\text{m}$, $80\ \mu\text{m}$, and $120\ \mu\text{m}$, which refers to a sample of macroscopic size. To obtain a phase-contrast image of the studied sample, the distance from the source to the center of the object was $R = 1\ \text{m}$, and from the center of the object to the screen $-\Delta = 2.7\ \text{m}$. The number of breakpoints for the wavefront after passing through the sample and for the screen were 845650 and 320400, respectively. Such a minimal division allows obtaining a sufficiently high-quality image of the object, but requires the calculation of about 10^{12} parameters according to the formula (10).

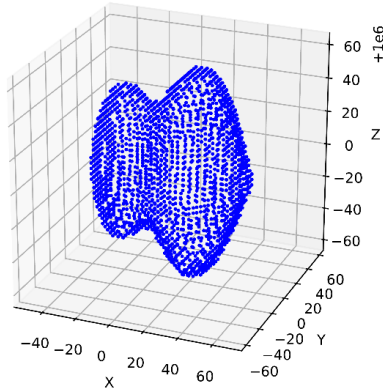


Fig. 3 – The research object with a maximum linear size of about $100\ \mu\text{m}$

Figure 4 shows the image of the sample and the spatial signal of the object for the angle 0° in the xy plane. This allows to see the contours of the object when looking at it along the z axis, and estimate the dimensions of the sample along the x and y axes.

Indeed, if we take into account that the coefficient of increase M in our case is equal to

$$M = 1 + \frac{\Delta}{R} = 3.7, \quad (13)$$

and determine the maximum size of the object on the graph in the Figure 4 as the distance between the points where significant oscillations begin and end in the central part of the graph (this is the sample location area), then we will get the following results.

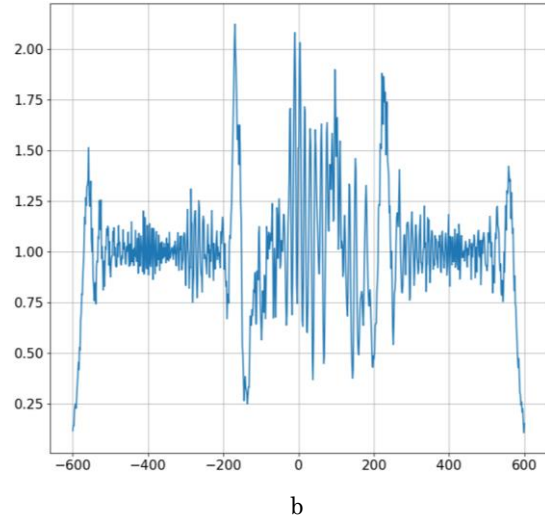
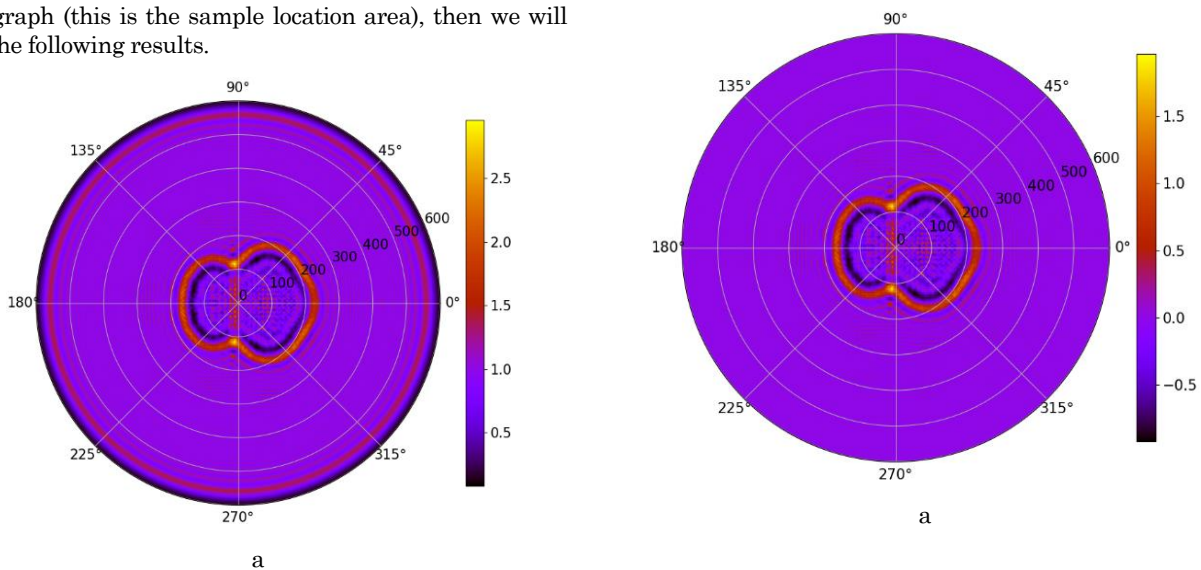


Fig. 4 – An image of the sample in the XOY plane and the object signal profile

The oscillations start approximately at the point $x_1 = -180\ \mu\text{m}$ and end at the point $x_2 = 220\ \mu\text{m}$. This means that the maximum dimensions of the image of the investigated object along the x axis are approximately equal to $400\ \mu\text{m}$, and therefore, taking into account the magnification factor (see the formula 13), the real size of the object along the x axis is approximately $108\ \mu\text{m}$. It can be assumed that this approximate calculation is fully consistent with the real size of the investigated object equal to $100\ \mu\text{m}$ along the x axis.

As for the information about the thickness of the studied sample along the direction of propagation of X-rays, we cannot determine this information directly from the data shown in the figure 4. To solve this problem, it is necessary to construct the image of the sample and the spatial signal of the object using the relative signal intensity (the difference between the signals with and without the sample) as shown in the figure 5. This allows you to exclude the influence of diffraction maxima and minima from the edges of the aperture and reduces oscillations, which makes it possible to more accurately determine the contours of the object under study.



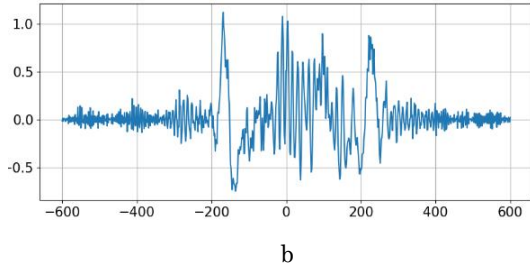


Fig. 5 – An image of the sample in the XOY plane and the object signal profile

In our research, we chose a sample with a small refractive index $\delta = 10^{-6}$, which corresponds to biological objects. To obtain more accurate information about the geometric shape and thickness of the object under study, we calculated the phase profile and constructed an image (Figure 6).

This result shows that our X-ray diffraction simulation parameters for the selected sample are correct.

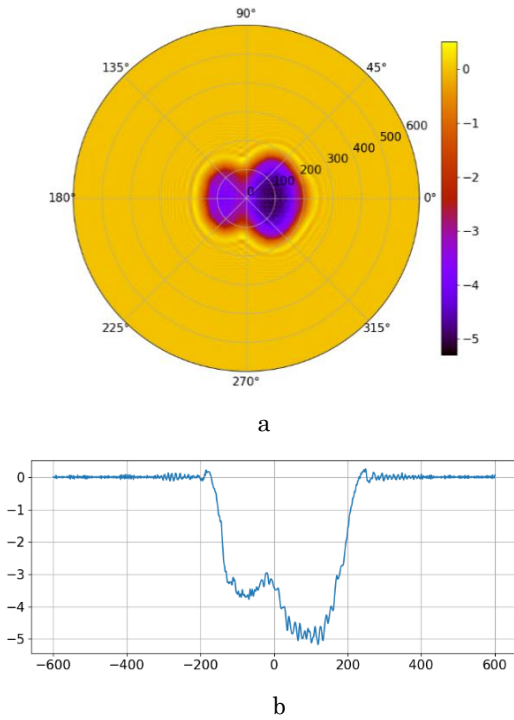


Fig. 6 – An image of the sample in the XOY plane and the object signal profile

Based on the calculated complex amplitudes of the previous images (with and without the object), the X-ray phase value was found for each case and their difference was found. In this way, the spatial distribution of the X-ray phase shift caused by the object was calculated. It should be noted that the detectors can only register the intensity and cannot register the phase of the X-ray radiation.

That is why the collection of data on the intensity and phase of radiation gives more complete information about the studied objects. Comparing the image intensity data in different areas and the phase profile graph with the geometric shape of the sample (Figure 3), we see complete correspondence.

The approach of modeling the interaction of X-ray radiation with matter proposed in this paper is suitable not

only for biological objects. It can also be used for crystalline structures, for example, metals and their alloys. But for metallic samples, we cannot neglect the absorption coefficient β . In addition, the refractive index δ and the absorption coefficient β for metals are very sensitive to changes in the electron density of the material. We will show this on the example of the phenomenon of thermal expansion of Fe-Cr-Al alloys. The parameters of crystal lattices at different temperatures and concentrations of components were calculated by molecular dynamics methods using the LAMMPS [28] package (see Table 1).

Table 1 – Crystal lattice parameters a [Å] for Fe-Cr-Al alloys at different temperatures and component concentrations

	300K	500K	600K	700K	800K
Fe-13%Cr-2%Al	2.8450	2.8505	2.8532	2.8560	2.8586
Fe-13%Cr-4%Al	2.8497	2.8551	2.8578	2.8604	2.8630
Fe-13%Cr-6%Al	2.8546	2.8599	2.8625	2.8648	2.8676
Fe-13%Cr-8%Al	2.8593	2.8645	2.8671	2.8695	2.8721

Also, for the calculations of δ and β , we used the values of atomic form factors, which are shown in the 2 [24] table, for pure metals.

Table 2 – Order numbers z , atomic form factors f_1 and f_2 , optical refraction decrements δ and absorption coefficients β for X-ray radiation with a wavelength $\lambda = 1.5374$ Å (line CuK_α) for some pure metals [24]

Parameter	Chemical element		
	Fe	Cr	Al
z	24	26	13
$f_1 = z + f'$	24.88	23.85	13.21
$f_2 = f''$	3.199	2.423	0.2406
$\delta \cdot 10^5$	2.2391	2.1055	0.84366
$\beta \cdot 10^6$	2.8793	2.1387	0.15364

Using the formulas (6) and (8), the refraction decrements δ (see table 3) and absorption coefficients β of Fe-Cr-Al alloys were calculated (see Table 4).

Table 3 – Refractive indices $\delta \cdot 10^5$ for Fe-Cr-Al alloys at different temperatures and concentrations of components

	300K	500K	600K	700K	800K
Fe-13%Cr-2%Al	2.2569	2.2438	2.2375	2.2309	2.2248
Fe-13%Cr-4%Al	2.2243	2.2117	2.2055	2.1995	2.1935
Fe-13%Cr-6%Al	2.1916	2.1795	2.1735	2.1683	2.1619
Fe-13%Cr-8%Al	2.1597	2.1479	2.1421	2.1367	2.1309

Table 4 – Absorption coefficients $\beta \cdot 10^6$ for Fe-Cr-Al alloys at different temperatures and concentrations of components

	300K	500K	600K	700K	800K
Fe-13%Cr-2%Al	2.7979	2.7818	2.7739	2.7657	2.7582
Fe-13%Cr-4%Al	2.7299	2.7144	2.7068	2.6994	2.6920
Fe-13%Cr-6%Al	2.6619	2.6472	2.6400	2.6336	2.6259
Fe-13%Cr-8%Al	2.5952	2.5811	2.5741	2.5676	2.5606

From the obtained results, we can conclude that with an increase in temperature due to thermal expansion, the parameters of the crystal lattice of the studied samples increase and, accordingly, the values of δ and β decrease, which can be fixed by changing the diffraction patterns of X-ray radiation.

5. CONCLUSIONS

In this work, we proposed a new approach of modeling X-ray diffraction on three-dimensional models of macroscopic objects of arbitrary shape, which allows more accurate calculation of the thickness of the studied samples in comparison with the works of other authors. The possibility of obtaining clear images of objects with low refractive indices, determining their geometric dimensions and thickness was demonstrated by the

method of phase X-ray contrast. Using the methods of molecular dynamics and known theoretical ratios, a methodology for calculating the refraction decrements and X-ray absorption coefficients for multicomponent metal alloys is proposed. The approaches presented in this work can be useful to developers of compact devices for detecting structural inhomogeneities inside the studied objects by a non-destructive method.

ACKNOWLEDGMENTS

The work was supported by the state research project № 0122U000417 and the Grant of the NAS of Ukraine 2024-2025 y. of research groups of young scientists № 0124U002466 and the Associated International Laboratory LIA/IRP IDEATE.

REFERENCES

1. M. Endrizzi, *Nucl. Instrum. Meth. Phys. Res. Sect. A* **878**, 88 (2018).
2. Y.S. Kashyap, P.S. Yadav, T. Roy, P.S. Sarkar, M. Shukla, A. Sinha, *Appl. Radiat. Isot.* **66** No 8, 1083 (2008).
3. A. Bravin, P. Coan, P. Suortti, *Phys. Med. Biol.* **58** No 1, R1 (2012).
4. T. Tuohimaa, M. Otendal, H.M. Hertz, *Appl. Phys. Lett.* **91** No 7, 074104 (2007).
5. A. Snigirev, I. Snigireva, V. Kohn, S. Kuznetsov, I. Schelokov, *Rev. Sci. Instrum.* **66** No 12, 5486 (1995).
6. K.A. Nugent, T.E. Gureyev, D.F. Cookson, D. Paganin, Z. Barnea, *Phys. Rev. Lett.* **77** No 14, 2961 (1996).
7. R.A. Lewis, *Phys. Med. Biol.* **49** No 16, 3573 (2004).
8. F. Arfelli et al., *Phys. Med. Biol.* **43** No 10, 2845 (1998).
9. S. Tao, C. He, X. Hao, C. Kuang, X. Liu, *Appl. Sci.* **11** No 7, 2971 (2021).
10. A. Momose, *Phys. Medica* **79**, 93 (2020).
11. D. Gabor, *Nature* **161** No 4098, 777 (1948).
12. S.W. Wilkins, T.E. Gureyev, D. Gao, A. Pogany, A.W. Stevenson, *Nature* **384** No 6607, 335 (1996).
13. A. Pogany, D. Gao, S.W. Wilkins, *Rev. Sci. Instrum.* **68** No 7, 2774 (1997).
14. A. Peterzol, A. Olivo, L. Rigon, S. Pani, D. Dreossi, *Med. Phys.* **32** No 12, 3617 (2005).
15. A. Burvall, U. Lundstrom, P. Takman, D. Larsson, H. Hertz, *Opt. Express* **19**, 10359 (2011).
16. S.C. Mayo, A.W. Stevenson, S.W. Wilkins, *Materials* **5** No 12, 937 (2012).
17. A.J. Carroll, G.A. van Riessen, E. Balaur, I.P. Dolbnya, G.N. Tran, A.G. Peele, *J. Opt.* **19** No 7, 075003 (2017).
18. D. Paganin, *Coherent X-Ray Optics* (Oxford University Press, 2013).
19. D.M. Paganin, D. Pelliccia, *Tutorials on x-ray phase contrast imaging: Some fundamentals and some conjectures on future developments*. arXiv:1902.00364 (2019).
20. D. Paganin, S.C. Mayo, T.E. Gureyev, P.R. Miller, S.W. Wilkins, *J. Microsc.* **206** No 1, 33 (2002).
21. D. Paganin, K.A. Nugent, *Phys. Rev. Lett.* **80** No 12, 2586 (1998).
22. P.C. Diemoz, A. Bravin, P. Coan, *Opt. Express* **20** No 3, 2789 (2012).
23. B.L. Henke, E.M. Gullikson, J.C. Davis, *At. Data Nucl. Data Tables* **54** No 2, 181 (1993).
24. A. Olivo, E. Castelli, *Rivista del Nuovo Cimento* **37**, 467 (2014).
25. O.M. Buhay, A.A. Drozdenko, M.I. Zakharets, I.G. Ignat'ev, A.B. Kramchenkov, V.I. Miroshnichenko, A.G. Ponomarev, V.E. Storizhko, *Physics Procedia* **66**, 166 (2015).
26. K. Dupraz et al., *Physics Open* **5**, 100051 (2020).
27. <https://www.lammps.org>.

Вивчення оптичних властивостей та структурних особливостей об'єктів методом рентгенівського фазового контрасту

А.Ю. Овчаренко, О.А. Лебедь

Інститут прикладної фізики Національної академії наук України, 40007 Суми, Україна

Фазовий контраст знаходить широке застосування в усіх галузях, де потрібна візуалізація внутрішньої структури об'єктів за допомогою рентгенівського випромінювання. У роботі запропоновано новий підхід моделювання фазоконтрастного рентгенівського зображення методом вільного поширення на основі теорії Френеля-Кірхгофа. Розроблена проста розрахункова модель дозволяє визначити значення зміни інтенсивності на тривимірних моделях об'єктів макроскопічних розмірів довільної форми і, відповідно, умови спостереження контрастного зображення при відомих характеристиках детекторної системи та інтенсивності джерела випромінювання. Була показана можливість одержання чітких зображень об'єктів з малими декрементами заломлення, визначення їх геометричних розмірів та товщини. Розроблено підхід розрахунку оптичних властивостей металевих сплавів у рентгенівському діапазоні. Викладені у роботі підходи можуть бути корисні розробникам компактних пристроїв для виявлення структурних неоднорідностей всередині досліджуваних об'єктів неруйнівним методом.

Ключові слова: Рентгенівський фазовий контраст, Взаємодія випромінювання з речовиною, Неруйнівний аналіз, Рентгенівська дифракція, Теорія дифракції Френеля-Кірхгофа, Внутрішня структура, Теплове розширення